Journal of Applied Physics ARTICLE pubs.aip.org/aip/jap

The role of sample–window coupling in shock temperature experiments

Cite as: J. Appl. Phys. **138**, 075902 (2025); doi: 10.1063/5.0277627
Submitted: 24 April 2025 · Accepted: 18 June 2025 ·
Published Online: 18 August 2025

T. M. Hartsfield,[1,a] K. M. Amodeo,[1,a] D. Ramsey,[2] D. J. Buckley,[2] L. R. Veeser,[3] and D. H. Dolan[1,4,a]

AFFILIATIONS

[1]Sandia National Laboratories, Albuquerque, New Mexico 87185, USA
[2]Nevada National Security Sites, Sandia Operations, Albuquerque, New Mexico 87185, USA
[3]Nevada National Security Sites, Los Alamos Operations, Los Alamos, New Mexico 87544, USA
[4]Institute for Shock Physics, Washington State University, Pullman, Washington 99164, USA

[a]**Authors to whom correspondence should be addressed:** thartsf@sandia.gov; kmamode@sandia.gov; and ddolan@wsu.edu

ABSTRACT

Radiometric studies of opaque materials under shock compression probe a sample–window interface that may be very different than the bulk state. Subtle experimental details, particularly an initial sample–window gap vs an adhesively bonded stack, have tremendous influence on measured temperature. This work experimentally tests gapped vs bonded targets and theoretically investigates observed differences in the measured temperature. The results indicate that perturbations created by a thin adhesive are smaller than those suggested by a previous work, whereas sample–window gaps alter the measured state more significantly than that previously realized.

I. INTRODUCTION

Temperature measurements are crucial to defining various states—such as shock, release, and reshock—created by dynamic compression.[1,2] Spectral radiance measurements have been used to infer temperature in such experiments for nearly 60 years.[3–8] For initially transparent samples, the radiant surface is an opaque shock front emitting through an upstream ambient material.[3,5,9–12] Different approaches must be used for opaque materials, such as metals. The samples can be shocked and subsequently released into vacuum and/or rarefied atmospheres,[13–16] but the nature of the emitting surface can be challenging to interpret.[15,17] These measurements intrinsically bring the sample to zero pressure, obscuring knowledge of the dynamic compression state.

Attaching a transparent window to an opaque sample maintains nonzero stress at the measurement interface.[6,18–21] Very often, this window is lithium fluoride (LiF), which is thought to remain transparent for pressures below 200 GPa.[22] Since the window's mechanical impedance rarely matches the sample under study, pressure at the sample–window interface is different (usually lower) than the original bulk state. Sample temperatures are, thus, modified by the use of a window. Instead of the shock state, the experimentally accessible condition is a shock-release state. This distinction is not unique to radiometry measurements: velocimetry measurements are subject to the same perturbation.

Details of the sample–window configuration substantially impact measured radiance in shock-loaded samples. Although mechanical states (velocity, pressure, and density) are largely insensitive to these subtleties, temperature is extremely dependent on them. This work considers several designs for measuring temperature under dynamic compression. Discussion begins with a survey of the previous results using one of the four basic designs. This is followed by discussion of a campaign of experiments testing bonded sample–window configurations and comparing them to gapped configurations. The results provide insight about the working range of optical adhesives under dynamic compression, demonstrate differences between bonded and gapped experiments, and confirm fundamental challenges with gapped experiments. Finally, a summary of conclusions drawn from this work is presented with recommendations for future radiometry studies.

II. TARGET CONFIGURATIONS

Figure 1 shows several implementations (not to scale) of an opaque sample backed by a transparent window in a plate impact experiment. Configuration (a) creates direct contact after shock, prior to which there is a finite gap between the two solid materials. Configuration (b) is a variation of configuration (a), where a thin film is deposited onto a window separated from a bulk sample of the same (nominal) composition. Configuration (c) is an altogether different approach, where an adhesive—a single-component glue or two-component epoxy—couples the window to the sample. Configuration (d) dispenses with the intermediate sample, launching the material of interest directly onto a window (typically coated with an emissive film).

A. Gapped experiments

Attaching a window to an opaque sample without an intermediate layer—i.e., mating two solid surfaces with finite roughness and radius of curvature as in Fig. 1(a)—always leaves some residual gap. The flatness and surface roughness common in commercial pieces, even when supplemented with additional polishing, is limited by material surface properties (such as adhesion of impurities and galling), material strength (fracture limits), tool/fixture flatness over many millimeters of travel, and further factors. These factors practically limit sample–window gaps to approximately 1 μm or greater. The precise gap thickness in previous works is largely unknown, though characteristic values are 1–20 μm: smaller values are difficult to verify, and larger values would presumably be apparent in cumulative thickness measurements. Such gaps are readily closed by shock compression, where stresses are much larger than the strength of either solid.

The overall gap fluctuations and/or lateral gap variations (e.g., center to edge) may explain why previous works using configuration (a) seem to resist simple analysis. Poulsen *et al.* stated that gaps and irregularities at the sample–window interface gave rise to flashes.[23] Huang *et al.* pressed transparent samples to LiF windows and reported very large quantities of radiance that decayed over time; they attributed it to flash and localized high temperature.[24]

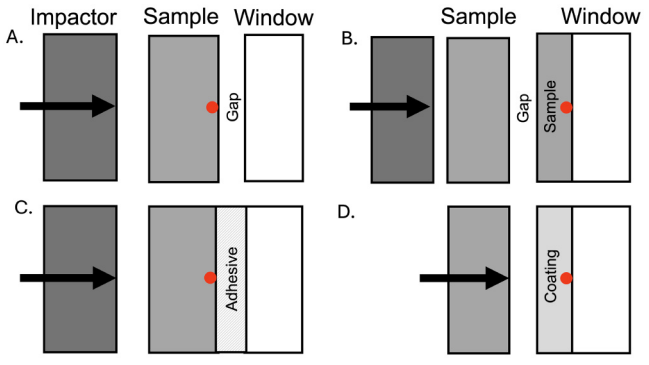

FIG. 1. Experiment configurations for measuring sample radiance through an optical window. Red dots indicate the primary emitting surface.

Hao *et al.* measured radiance from targets pressing a copper plate directly to a sapphire window.[25] Despite reporting on the copper temperature, their measurements were certainly compromised by the absorption and emission of shocked sapphire.[26–28] Liu *et al.* reported a successful measurement using a clamped sample, but gave no details about the gap thickness or uniformity.[29] Li *et al.*[30] and Zhang *et al.*[31] reported similar measurements on iron (Fe) and vanadium (V), respectively. Li describes the window–target direct attachment via clamping, while Zhang used a similar configuration and polished the samples but did not elaborate on the attachment method or the gap thickness. La Lone and colleagues clamped a slightly bowed Fe sample to a window, observing optical fringing between the sample surface and the window to infer a gap at the center of a similar or smaller extent than the ~700 nm test light.[28] As a transmitted shock exited Fe, that material released into the gap, contacted the window, and reshocked against LiF. The optical signal increased, peaked, and relaxed through the duration of the experiment. They attributed this to a combination of a non-thermal optical flash and the heating and subsequent diffusion of heat from the reshocked material near the interface. Hydrodynamic simulations of the experiments suggested that even gaps smaller than 1 μm generate substantial localized heating and diffusion, in addition to the potential optical backgrounds. Data reported by La Lone, Li, Liu, and Zhang show decaying temperature in all shots, with relative decrease varying from 5% to 40% in different experiments over the duration of the steady shock pressure.

Configuration (b) (Fig. 1) moves the physical gap in a clamped sample away from the measurement interface, although doing so raises questions about the density and structure of the coating sample vs its bulk companion. Williams, Bass, and, later, Tang sputtered Fe onto an optical window and pressed the sputtered Fe against a solid Fe baseplate, through which a shock was transmitted.[18,32,33] These studies reported the calculation of apparently sensible shock state temperatures in metals through complex analysis and modeling. Yet, many of these measurements were almost certainly invalidated by the loss of transparency in, and optical emission from, the shocked sapphire window[26–28] and the loss of transparency in LiF above approximately 200 GPa.[22,34] Yoo *et al.* attempted the same experiment using a diamond window to study iron.[6] The shock states and melt temperatures inferred from these experiments were, in general, anomalously high compared to the data measured under static high pressure, calculated theoretically, or inferred from shock measurements and EOS calculations,[35–38] and many subsequent studies disregard them. Svendsen and colleagues attempted with limited success to analytically investigate the thermal diffusion across sample-coated film–window interfaces from the data of Bass.[39] A recent work by Brantley applied Svendsen analysis to the new data taken in this configuration, finding similar difficulty in matching experimental results.[40] Dai *et al.*[41] measured radiance from a target consisting of a Ta film coated onto LiF, pressed against a Ta driver, and shocked to 300–400 GPa. Their analysis of the Ta bulk shock state inferred Ta melt values approximately 3000–6000 K greater than those measured at static high pressure and calculated via theory; see Dewaele's discussion[42] for details. Dai *et al.* performed the same experiment on V.[43] Their reported temperatures were 1000–3000 K higher than those obtained by Zhang with the clamped V target.[31]

Among other issues, all but one of Dai's V experiments used a sapphire window that would have suffered from the loss of sapphire transparency.[41]

B. Bonded experiments

Shock experiments measuring interface velocity have used sample–adhesive–window bonding for decades.[44,45] Temperature measurements in this configuration were first successfully reported by Blanco *et al.*[19] Numerous studies have since employed this configuration.[7,8,20,21,46–50] Temperatures measured at the metal surface appear nearly steady under steady shock stress, increase under further compression, and decrease with pressure release. When emissivity is measured[49] or constrained by ambient measurements in combination with statistical or physical models,[51] the reported values are generally in sensible agreement with the models and static high pressure data.

This technique imposes certain limitations on radiance experiments. The adhesive must remain transparent under significant compression to pass emission from the sample, while also not emitting itself. Loctite 326 (hereafter Loctite) and Loctite 358 are the only adhesives experimentally known to remain transparent under certain compression conditions.[7,20,52,53] This is despite the experimental observation that polymers generally decompose at roughly two times the ambient solid density (20–30 GPa).[54]

Although attaching a sample directly to a window via diffusion bonding is a promising concept, no successful temperature measurements of such a shocked system have been reported. The processes needed for successful diffusion bonding are difficult and often create layers of differing local density, grain structure, and void fraction. Bonding may also require adding layers of other materials near the measurement interface, complicating the measured state.[55]

C. Direct impact

In theory, direct impact is the simplest possible sample–window interface, particularly if the window coating shown in Fig. 1(d) can be omitted. Doing so accesses the principal shock (Hugoniot) state, rather than the reflected states created in all other configurations. However, the residual atmosphere gathered along the projectile's flight path creates an intense impact flash that blinds radiometric instruments. For example, Boness reported a flash several-fold brighter than the emission from a ∼4000 K emitter.[56] Coating the window reduces, but does not entirely eliminate, residual gas flash in direct impact. La Lone and colleagues reported substantial impact flash measured through a 150 nm thick Cr layer.[57] A thicker opaque coating applied to the window did shield this flash but substantially complicates the measurement interface. Hartsfield *et al.*[58] reported direct impact experiments using coated windows and found that temperature at the window–coating interface was substantially different from that of the impactor (sample) Hugoniot state. They concluded that temperature at the measurement interface was dictated by thermal diffusion of the layers of heat created by the pressure equilibration of the short-lived stress states in a "Reverberation Affected Zone" (RAZ) across the interface. Generally, the interface temperature could not be simply related to the Hugoniot state temperature of the coating, impactor, or window. Extrapolating from this interface temperature to the temperature away from the interface, as demonstrated by Svendsen, Tang, Brantley, and others, is extremely difficult. While the interface affects the cloud determination of a bulk thermodynamic state of the shocked sample, local interface states measured directly may be useful by themselves. For instance, isobaric heating and cooling at the interface can be used to locate phase boundaries such as melt.[59]

III. EXPERIMENTAL METHODS

This work studied both gapped and adhesive-bonded interfaces under shock compression in a series of two-stage light-gas gun experiments at the Shock Thermodynamics and Applications Research (STAR) facility at Sandia National Laboratories. Each experimental target was prepared and characterized in the same manner before the experiment. All experiments employed a common measurement design, allowing direct comparisons between the results.

A. Concept

Figure 2 illustrates the "Firefly" design. In each experiment, a two-stage gas gun accelerated a Ta flyer to an impact velocity between 2.78 and 6.03 km s^{-1}; the flyer impacted an Al baseplate backed by a series of single-crystal LiF pieces oriented along the [100] axis and polished to optical finish. Surface heights were measured to vary by a few μm across most pieces. The machined surface of the Al baseplate, to which the LiF pieces were attached, was lapped with 1 μm grit compound in most experiments. Each experiment injected laser light and collected Doppler-shifted backscatter (PDV)[60] and thermal emission (pyrometry) from the Al front surface.

Measured emission from the Al–LiF interface began at shock breakout (sbo). The steady Al–LiF interface emission created a backlight to test the transparency of the downstream stack of LiF pieces and the interfaces between them. Failure of an interface, for radiometric purposes, was indicated by the changes of Al radiance

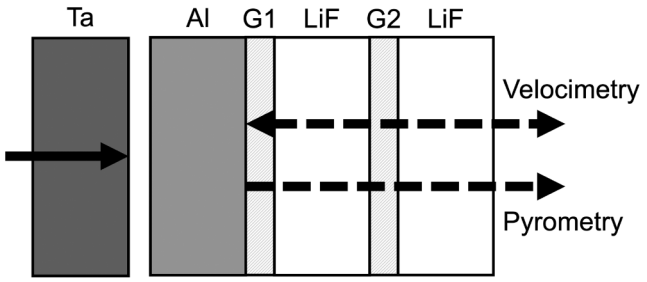

FIG. 2. A schematic of the experiment testing interfaces under shock. A shock wave driven through an Al baseplate by a Ta impactor crosses an adhesive bond or gap (G1), transits LiF, and crosses a second bond or gap (G2) into another LiF crystal. Some experiments added a third window and interface. PDV and pyrometry measure continuous interface velocity and emission at the Al–LiF interface. Bonds/gaps are shown much thicker than they truly are for visual clarity.

signal beginning when the shock reached that interface. The nature of radiance from, and apparent temperature of, the Al–LiF interface also provide insight into the compressed sample–window interface. Most experiments tested the adhesive Loctite at this interface, while some experiments tested an evacuated gap.

The apparent sample–window interface temperature T determined in each experiment was used in several ways. For bonded samples, excessively large values (relative to thermodynamic calculations for Al) were considered an evidence of the possible adhesive failure. For gapped samples, comparisons were made to both calculated temperatures and experimental measurements from bonded samples at similar pressure. Absolute differences in T also provide contrast between the bonded and gapped samples compressed to similar pressures. In all instances, the time dependence of T revealed trends in thermal diffusion between the sample and the optical window.

B. Target design, assembly, and metrology

The first LiF window, with noted exceptions, was bonded to the Al baseplate using Loctite. A second LiF window was attached to the first with another adhesive to be tested. In some experiments, a third LiF window was bonded to the back surface of the second. Each bond, with noted exceptions, was created using a standardized pressing process. Prior to application, the adhesive was held in a chamber evacuated to ∼130 Pa (∼1 Torr) until all bubbling ceased. Some assemblies did not vacuum de-bubble Loctite, as large bubbles formed at the surface of the highly viscous glue, a possible indication of boiling. Adhesive was spread finely on one piece (sample or window), the second piece was placed in contact with the covered surface, and then, the stack was manually pressed until the adhesive spread completely across the interface. The attached pieces were then placed in a mechanical press under the highest pressure possible, at least 400 kPa, across the surface area of the sample, and left until fully cured. Two of the experiments tested a gapped interface, created by pressing two windows without an intermediate bond and then tacking the pieces together with epoxy around the circumference, described in Sec. IV B. All experiments employed optical shielding to mask the pyrometry measurement from outside light: the samples were surrounded by an Al ring, topped with an Al washer, and black epoxy or black paint was applied to fill all accessible mating surfaces.

Loctite (without an additional activator) cure is frustrated by the lack of contact with a metal surface. Tests of the LiF–Loctite–LiF samples showed a very gradual curing. At 1–3 days, the glue was not fully hardened. After one week, the glue bond no longer yielded under mechanical shear. The LiF–Loctite–LiF bonds in the targets were tested with cure times of approximately one month and one week. In each case, the adhesive layers were as thin as reasonably possible. The experimental tests showed no measurable difference between the LiF–Loctite–LiF bonds cured for one week and for one month.

Bond and gap thicknesses in each sample stack were measured with a white light interferometer. Using a design similar to that described by Marshall,[61] broadband light from a single-mode optical fiber was focused onto the interface between two successive pieces. Interference between waves reflected from the surface at each side of the interface created fringe patterns[62] in the spectrum of the collected light. The frequency of the interference pattern indicated the imparted phase shift, allowing determination of the optical path length through the bond/gap.

C. Radiometric measurements and analysis

Sample radiance was measured using four independent radiometry detectors, using bandpasses with center wavelength (full width) of 980(10), 1225(50), 1425(50), and 1600(50) nm. After the final hookups were made, the detectors were calibrated by measuring the total band-averaged spectral radiance from a calibrated blackbody source, transmitted through the complete optical probe for each experiment. Radiometric analysis was performed as described in a previous work;[51] the calculations were implemented using the RadiometryAnalysis class in the SMASH analysis package.[63]

Temperatures ascribed to the radiance measurements are estimates for comparison purposes only and not intended to carefully constrain the true thermodynamic temperature of the shocked samples. In each case that an aluminum surface T was estimated, the calculations were performed identically from radiance collected at 1425 nm, with an estimated emissivity of 0.2.[29] No corrections for shock history, glue temperature, LiF temperature, thermal diffusion, optical effects at elevated (T, P), or other factors were attempted. Comparisons between experimentally estimated T and theoretically calculated T use a well-regarded multi-phase Al EOS published by Sjostrom *et al.*[64]

IV. RESULTS

Seven two-stage gun experiments, named Firefly (FF) 1–7, tested 17 interfaces of varying designs between 46 and 136 GPa. The experimental configurations and results are summarized in Table I. Characteristic results from these experiments are shown below.

A. Bond transparency under dynamic compression

Figure 3 demonstrates the glue transparency test results from two experiments. The first experiment (left) shows failure, while the second (shifted right) shows no failure in two bonds. Several common adhesives in shock research were tested in addition to Loctite 326: ÅngströmBond AB9110LV, EPOTEK 301-1, and Loctite Stycast 1266 A/B, hereafter referred to as AngstromBond, Epotek, and Stycast, respectively. Table I lists the result of each bond transparency test. Complete transparency of LiF—retaining ambient bulk transparency, a much more stringent condition than allowing some velocimetry return, required for accurate pyrometry—was seen at stresses up to 136 GPa on the solid LiF Hugoniot.

B. Gapped interface tests

Three experiments tested the gapped interfaces. White light interference measurements prior to each experiment indicated a substantial gap variation. The initial LiF–LiF gap in Firefly 1 decreased monotonically toward the center of the interface: it was 4.9 μm thick at a radius $r = 18$ mm from the center, 1.4–4.1 μm at $r = 15$ mm, 1.1–3.0 μm at $r = 10$ mm, and ≤ 1 μm at $r \leq 5$ mm from the center. Firefly 6 and 7 employed gaps between the Al baseplate and the first LiF window. The measurements of Firefly 6 indicated a gap thickness of between 3 and 7 μm, varying with position, while the measurements of Firefly 7 determined a gap thickness of

TABLE I. Summary of the Firefly experiments and results of the shocked glue transparency tests.

Shot number	Target stack	Thickness (μm)	Debubbled?	Est. initial P[a] (GPa)	Final P (GPa)	Bond failure?
Firefly 1	Al–Loctite–LiF	12	No	22	45.8 ± 0.5	No[b]
	LiF–Gap–LiF	≤1			45.8 ± 0.5	—
Firefly 2	Al–Loctite–LiF	3	Yes	33	76.0 ± 0.8	no[b]
	LiF–Epotek–LiF	5	Yes	33	76.0 ± 0.8	No
Firefly 3	Al–Loctite–LiF	3	No	55	107 ± 1.1	Likely[b]
	LiF–Stycast–LiF	9	Yes	55	107 ± 1.1	No
Firefly 4	Al–Loctite–LiF	5	Yes	73	136 ± 1.4	Likely[b]
	LiF–AngstromBond–LiF	3	Yes	73	136 ± 1.4	Yes
Firefly 5	Al–Loctite–LiF	2	No	31	66.5 ± 0.7	No[b]
	LiF–Epotek–LiF	14	Yes	31	66.5 ± 0.7	No
	LiF–Epotek–LiF	6	No	31	66.5 ± 0.7	No
Firefly 6	Al–Gap–LiF	3–7			100 ± 1.0	—
	LiF–Loctite–LiF (1 mo. cure)	6	No	52	100 ± 1.0	No
	LiF–Loctite–LiF (1 wk. cure)	5	No	52	100 ± 1.0	No
Firefly 7	Al–Gap–LiF	25			76 ± 0.8	—
	LiF–Loctite–LiF	10	No	33	76 ± 0.8	No
	LiF–AngstromBond–LiF	8	Yes	33	76 ± 0.8	No

[a]Estimated polymer first shock.
[b]Transparency inferred from Al–LiF radiance history.

25 μm. In each case, the LiF windows were tacked around approximately two-thirds of the exterior circumference, leaving space for gas within the gap to vent into the experiment chamber vacuum.

Figure 4 shows results from the Firefly 1 test, where no measurable change was observed as the shock closed the gap between two LiF windows at 46 GPa. Firefly 6 used a 4.91 km s^{-1} Ta impactor to shock Al to 102 GPa. This Al was then released to vacuum and reshocked to 100 GPa upon impact with LiF; Firefly 7, with a 4.03 km s^{-1} Ta impactor, achieved 77 GPa in Al on shock and 76 GPa upon Al–LiF equilibration. Figure 5 shows the results. Radiance levels and the estimated temperature rapidly decreased after shock breakout; Firefly 6 reached a nearly steady value, while Firefly 7 did not.

V. DISCUSSION: ADHESIVE BOND FAILURE

Adhesive bond failures have been reported in a previous work[53] as dramatic changes in measured radiance upon shock of the bond layer. One experiment shocking AngstromBond to

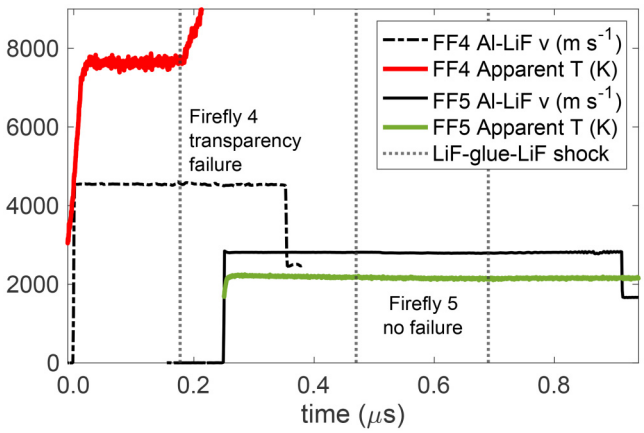

FIG. 3. Velocimetry and estimated temperature for Firefly 4 (left) and Firefly 5 (shifted 250 ns) experiments, demonstrating bond transparency and failure.

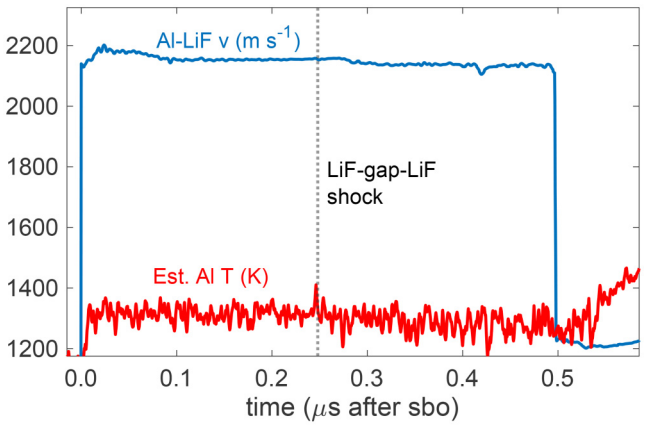

FIG. 4. Estimated Firefly 1 Al temperature is steady and there is no disturbance in radiance as the 46 GPa shock crosses the LiF–gap–LiF interface.

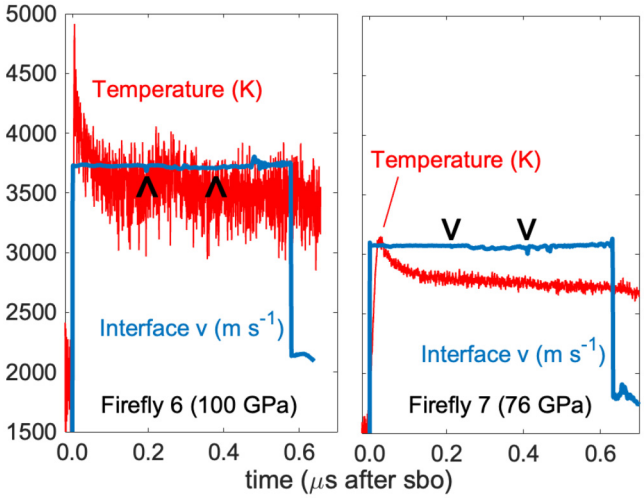

FIG. 5. Thermal histories at the Al–gap–LiF interface in two experiments. Glue bond transits without failure are denoted with arrowheads. Firefly 6 data are unfiltered to preserve high-frequency cooling. FF 7 had a larger sample–window gap than FF 6.

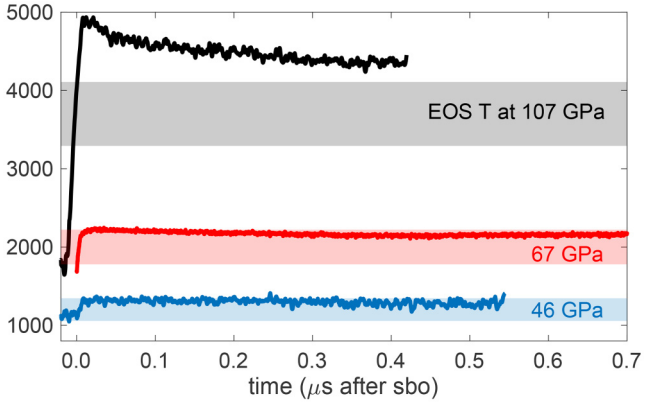

FIG. 6. Interface velocity and estimated interface temperature of shocked Al–Loctite–LiF bonds measured in three Firefly (FF) experiments. Shaded regions estimate shock temperatures at each pressure, assuming 10% uncertainty from the equation of state predictions.

136 GPa (Firefly 4, Fig. 3) yielded such an event. Seven experiments, measuring nine LiF–bond–LiF interfaces with equilibrium stresses between 46 and 107 GPa, showed no significant disturbance in the backlighting radiance. This indicates that with proper assembly, such bonds would not compromise pyrometry measurements of an opaque sample. A key difference to be noted is the use of wavelengths >900 nm in this work, whereas previous studies generally operated at shorter wavelengths.

One hypothesis for bond failure is the retention of small bubbles in the adhesive. In principle, these bubbles crush and jet upon shock compression, creating localized areas of very high temperature and possible optical emission. However, our tests observed no measurable difference between layers that had undergone the debubbling process and those that had not. This is especially clear in the Firefly 5 results shown in Fig. 3, where an Epotek layer that had undergone debubbling and another that had not were subjected to the same shock wave. Furthermore, bubble effects would seem to be more likely from the mixing of a two-component epoxy, but no differences were observed between these materials and single-component Loctite glue. Perhaps, bubbles are expelled during the pressing process, if sufficient pressure is applied, or maybe any entrained bubbles are of sufficiently small volume to not emit measurable light under shock.

Another hypothesis for glue bond failure is that a sufficiently hot material in contact with the glue will initiate a reaction within the glue polymer, causing it to decompose and lose transparency. This could explain why Loctite shocked to 107 GPa between Al and LiF failed, while Loctite shocked to 100 GPa between two pieces of LiF did not fail in two tests. We note that no direct evidence of bond failure due to contact with shock-heated LiF was observed in this work. LiF temperatures under shock compression are not well bounded experimentally, but may be as high as 2000–2500 K,[65] substantially lower than Al at the same shock pressure.

The lack of a pre-shock signal for the intact bond makes sample–window bond failure more difficult to determine than for bonds between windows. Figure 6 demonstrates the estimated T vs interface velocity (which scales with P) across three similar experiments using Loctite between Al and LiF. The blue (Firefly 1) and red (Firefly 5) plots show experiments where $P \leq 67$ GPa. The estimated Al T varies reasonably with shock stress. Even using our simplistic emissivity assumptions and making no attempts to compensate for interface effects, it does not differ greatly from a high fidelity Al multiphase EOS.[64]

Firefly 4 (Fig. 3), shocking Al–Loctite–LiF to 136 GPa, yielded a steady T dramatically higher than other experiments or thermodynamic predictions, providing strong evidence that the Loctite layer failed. Firefly 3, shown in black in Fig. 6, tested the Al–LiF interface at 107 GPa. Apparent T jumped to a value higher than the EOS prediction and decayed by ~10% under steady stress. At 107 GPa, bond failure is likely.

VI. DISCUSSION: TEMPERATURE IN BONDED VS GAPPED EXPERIMENTS

This section compares observations from the Al–LiF interface in several Firefly experiments. Loctite was the only adhesive bond used for that interface. The results of Secs. IV and V indicate that there is no obvious reason to suspect that an epoxy bond would yield substantially different results. The term glue is used here to contrast adhesive bonded from gapped targets. Hardened acrylic glue will also be treated as functionally similar to PMMA in calculations and simulations.

Figure 7 compares glued vs gapped Al–LiF interfaces in otherwise similar experiments. Firefly 5 tested Al attached to LiF with a 2 μm bond. Under a steady shock of 67 GPa, nearly steady radiance indicated an estimated Al $T \sim 2200$ K at shock breakout, dropping

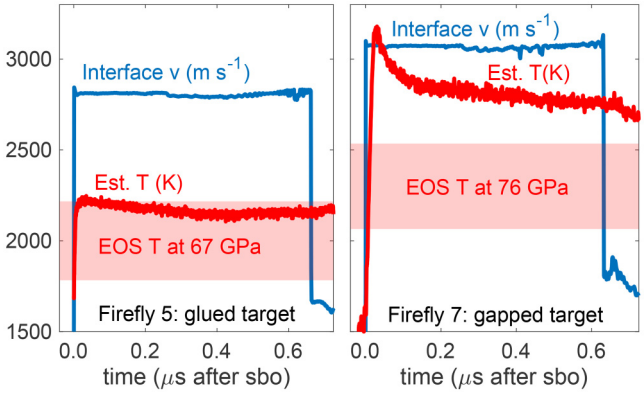

FIG. 7. Experimental sample–window interface velocity and temperature with shaded reference EOS T, for two similar experiments, with a glued (left) and a gapped (right) target. Shaded regions show 10% uncertainty in the calculated temperature.

to 2150 K; T varied by $\leq$50 K (2%). Firefly 7, with an evacuated gap between Al and LiF, saw dramatically decaying radiance. The estimated initial Al $T \sim 3150$ K at shock breakout dropped to 2800 K by the end of the experiment and never fully stabilized. Sjostrom's Al EOS suggests temperatures of 2000 K at 67 GPa and 2300 K at 76 GPa; the absolute T is not constrained by the published experimental data, but the relative difference of 300 K between the two Hugoniot states is a sensible estimate. The bonded experiment produced an estimated T less than 10%, different than theoretical T, while the gapped experiment, placing Al in direct contact with LiF at a much lower shock T, produced at the estimated T beginning 40% hotter and decaying to ~25% hotter. Firefly 6 saw an initial T approximately 1500 K greater than the EOS estimate; it cooled until reaching something close to the EOS estimation of ~3200 K. However, this interface temperature is not corrected by the methods described in Sec. 1 of Appendix A to account for cooling of the Al surface via thermal conduction into LiF. The corrections use interface T to estimate a lower bulk T, so the similarity of the interface and EOS T values in this instance is likely a coincidental arrangement of the factors described in Secs. VI A and VI B.

Radiance measured in a gapped experiment presumably varies from that measured in a glue-bonded experiment by three independent types of mechanisms. First, compression of any residual gas may create non-thermal emission, release of surface imperfections will create transient optical radiance from extremely hot jets, and other mechanisms may create localized variation in T. Second, thermal diffusion between the sample and the window will place the interface at a different state from the sample. Finally, T near the emitting surface will be dictated by a significantly different thermodynamic trajectory than that experienced by the glued samples.

The LiF–gap–LiF experiment (Firefly 1, Fig. 4) showed no substantial emission from compressed gas. Experiments testing shocked and released surfaces have found higher apparent T immediately after release, subsequently settling to a stable value, likely due to inversion and jetting of the localized surface geometry imperfections.[14–16] A free surface that does not impact another material, such as a window, and re-compress may see radiance evolution for tens or hundreds of nanoseconds. In Firefly 1, the surface was unloaded for 1 ns or less before impacting LiF, preventing measurable evolution of an expanding cloud of material. Any additional heating in the transparent LiF due to shock, release into the gap, and reshock upon the downstream LiF was not apparent in our diagnostics.

A. Thermal diffusion

The released material that crosses a gap and comes into direct contact with a window then experiences thermal diffusion. In most reports, a correction to estimate the sample temperature from the interface measurement is made using the model of Grover and Urtiew.[66] The model assumes infinite thermal conductance across the interface, resulting in a steady interface T. In practice, the observed temperatures steadily evolve over time, both in this study and the previous work. The details of that evolution strongly depend on the experiment configuration.

Appendix A describes the large uncertainties inherent in the conversion of the measured interface T to the bulk sample temperature. Both the estimation of thermal properties of the shocked materials and proper accounting for finite boundary conductance present independent uncertainties of order $\pm$10%−−20%. These uncertainties propagate forward with the adjustment for sample thermodynamic state history before the bulk temperature is determined. Thermal diffusion calculations that include boundary conductance are shown in Fig. 8 using relative temperature (1 for the sample, 0 for the window). Material near the sample surface lies at a value somewhere between those limits. Finite conductance supports a temperature discontinuity at the interface that gradually diminishes over time, although relaxation time scales can vary by several orders of magnitude. These trends are qualitatively similar to the gapped experiments: Firefly 6 and 7 (Fig. 5). For example, simulations using a range of plausible boundary conductance values predict an Al–LiF interface temperature decay of 3%–35% over the roughly 300 ns duration of a typical supported shock experiment.

At pressures of 46 GPa (Firefly 1) and 67 GPa (Firefly 5), radiance from the bonded sample is quite steady and consistent with the temperature predictions. This suggests that the bond is an extremely poor thermal conductor, allowing Al to maintain a very nearly steady shock T for at least several hundred nanoseconds. Figure 9 shows results of the calculations of thermal diffusion in a bonded experiment, detailed in Sec. 1 of Appendix A. The calculations indicate minimal diffusion through the sample–window bond and no substantial diffusion between the sample and the window over the time scales of shock experiments. The thermal stability of these simulations to <5% is consistent with experimental observations (Fig. 6, red and blue).

B. Thermodynamic states

Plots of pressure as a function of particle velocity (Fig. 10) are helpful in the comparison of different sample–window configurations; this particular illustration is based on the shock compression of aluminum to 100 GPa (dashed horizontal line). The black curve shows the lithium fluoride shock states derived from a tabular

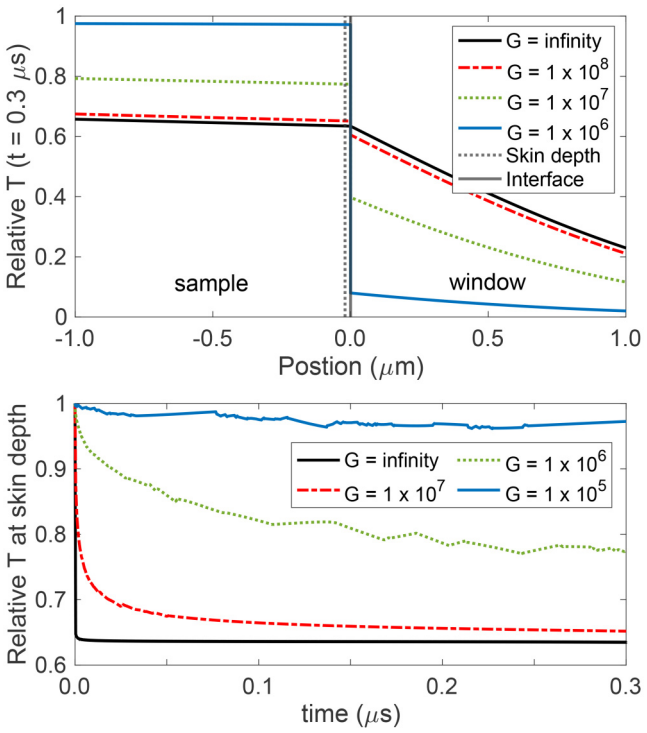

FIG. 8. Simulated relative temperature (sample = 1, window = 0) across an Al–LiF interface at $x = 0$ vs interface conductance G ($\mathrm{W\,m^{-2}\,K^{-1}}$). Top: $T(x)$ at 300 ns. Bottom: $T(t)$ at the Al skin depth.

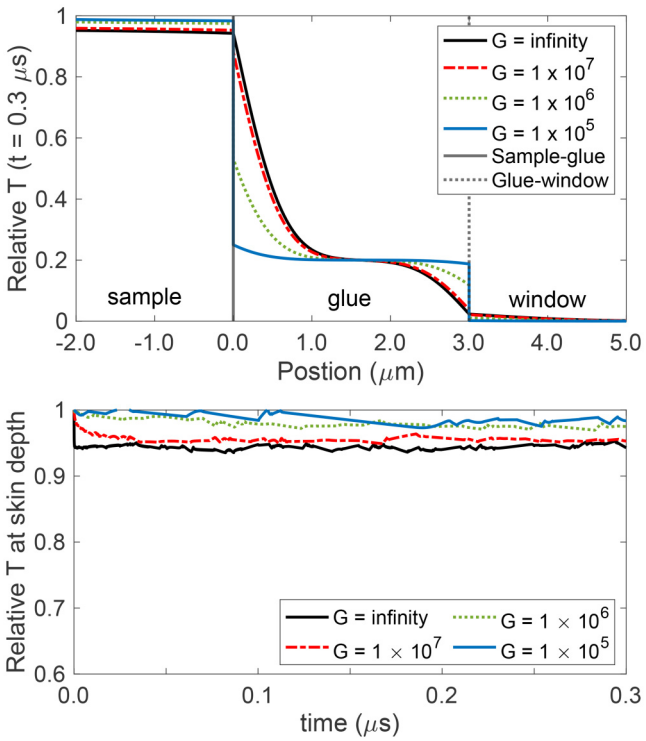

FIG. 9. Simulated relative temperature (sample = 1, glue = 0.2, window = 0) across an Al–glue–LiF interface vs interface conductance G ($\mathrm{W\,m^{-2}\,K^{-1}}$). Top: $T(x)$ at 300 ns. Bottom: $T(t)$ at the Al skin depth. Scales match Fig. 8.

equation of state (SESAME 7270). Sample (Al) shock states lie on the blue curve. Configuration (d) achieves the Al–LiF intersection state at the Al–LiF interface, but the same cannot be said for the other configurations. In the absence of a gap, the aluminum sample releases slightly to state 2a (97.5 GPa) due to the lithium fluoride window. For gapped configurations (a) and (b), the samples undergo complete release to zero pressure (2b), followed by reshock to a slightly different state pressure (95.7 GPa, state 3b at the Al–LiF intersection just below state 2a) than the original shock state; this progress is indicated by the mostly overlapping release (blue) and reshock (red) curves. Configuration (c) undergoes partial release to state 2c, defined by the intersection of the green curve representing adhesive shock states. Subsequent shocks across the bond restore pressure to the sample–window intersection near 100 GPa in a stepwise manner.

Both configurations expose the sample to shock compression, but

- gapped samples undergo *complete* release and reshock from $P = 0$ and
- bonded samples undergo *partial* release followed by multiple shock recompression.

The release in both configurations can be treated as nearly isentropic—shock waves are unstable for decreasing pressure, resulting in continuous (and nearly adiabatic) decompression.[1] However, the incompletely released sample in the presence of a bond layer retains a fair amount of enhanced stiffness from the original shock state; so the subsequent reverberation shocks do not

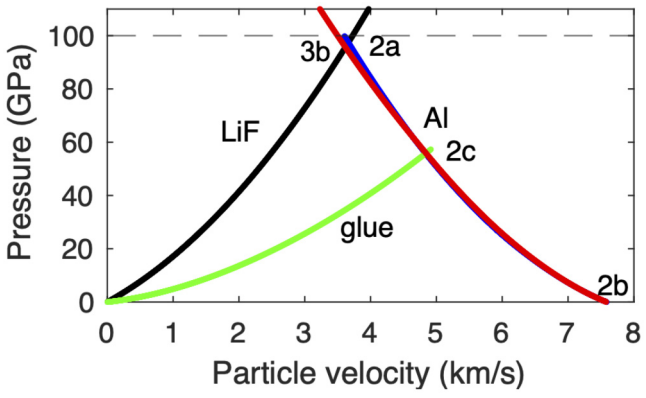

FIG. 10. Loading states for aluminum backed by LiF. The Al shock and release (blue) states and reshock states (red) are nearly identical.

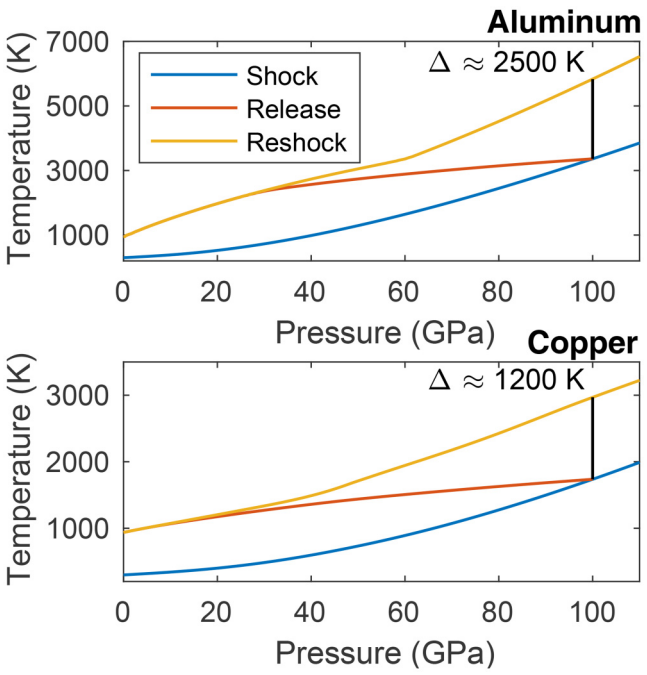

FIG. 11. Calculated shock (blue), release (orange), and reshock (yellow) temperature states for aluminum (top) used in this work and copper (bottom) as another example.

generate nearly as much density (or entropy) change as a shock from $P = 0$. To a very good approximation, recompression of the bonded sample follows the decompression path from 2c back to 2a, recovering the temperature of the sample–window intersection.

Reshocking a fully released sample results in a very different temperature state than reverberation. Figure 11 shows temperature calculations for aluminum and copper based on SESAME tables 93 722 and 3336, respectively. These calculations illustrate that samples exposed to full pressure release are substantially hotter than the original shock state upon recompression. Some of this increased temperature might diffuse into the window—this process is enhanced for gapped samples relative to bonded samples—but the fact remains that the observed sample temperature can be substantially higher than expected. Aluminum was used in the present experiments, but similar deviations would be observed in copper (as shown) or any other material of interest.

To quantify how much of a gapped sample is affected by the shock-release-reshock effects, consider the conceptual diagrams in Fig. 12. Just after the original shock reaches the sample–window gap (top), the free surface is launched toward the window. A continuous left-going release travels at sound speeds $|c_1| > |c_0'|$ from the high to the zero pressure domain, respectively. The free surface eventually strikes the window, creating a left-going reshock (3b, nearly equivalent to 2a), but the release has already been traveling for some time and fans out as shown (bottom). The minimum size

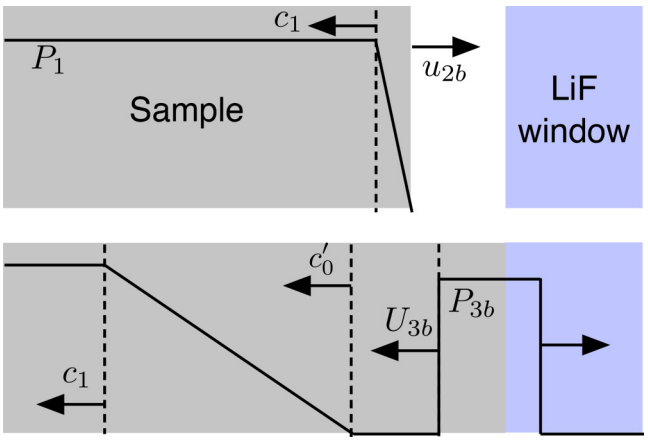

FIG. 12. Conceptual illustration of a gapped measurement just after shock release (top) and subsequent window impact (bottom).

of this release affected zone

$$h_{RAZ} > \frac{c_0}{u_{2b}}\left(\frac{U_s}{U_s - c_0}\right)h \approx \frac{c_0}{2u_1}\left(1 + \frac{c_0}{su_1}\right)h \tag{1}$$

depends on original gap thickness h, second shock velocity U_s (U_{3b}, about 10 km s^{-1} at $P_{3b} \sim 100$ GPa), and release particle velocity u_{2b} (about 7.6 km s^{-1}); the approximation is based on a linear material ($U = c_0 + su$) and the assumption that the release velocity is nearly twice the particle velocity. For this particular example, the RAZ is no less than $1.3h$, and this estimate only accounts for reshock overtake of the $P = 0$ state. Even in the limit of large particle velocity, h_{RAZ}/h can never be less than $c_0/2u_1$—in this case, roughly 0.6. The left edge of the release front travels roughly three times faster than the right edge, so the amount of material having undergone shock-release-reshock, experiencing some RAZ heating, is at least four times the gap thickness.

Figure 13 shows the results of 1D hydrodynamic simulations of gapped and bonded experiments created using the code CTH.[67] The simulations replicated the geometry of Firefly 6 and 7 experiments testing the Al–gap–LiF interfaces, the Firefly 5 Al–bond–LiF experiment, and the ideal case of a 1 μm gap. The experiments were slightly simplified by using a common impact velocity; this eases comparison without meaningfully changing the underlying physics. The effect of interface release is reflected in the temperature profile of aluminum after mechanical equilibration. Consistent with the calculations described above, Al near the interface experiencing the shock-full release-reshock process is heated to more than 3900 K, nearly twice the estimated bulk state temperature of less than 2300 K. The hottest layer width is one to two times the original gap thickness, with a tail extending more than 10× that distance.

The presence of a sample–window gap profoundly changes the temperature during shock compression. These differences persist over micrometer-scale distances. Given the characteristic

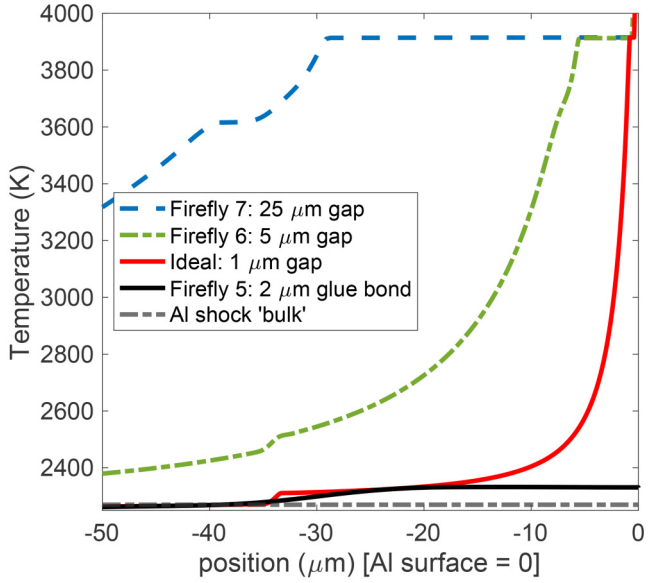

FIG. 13. Calculated $T(x)$ profiles for gapped and bonded experiments as conducted and in the ideal case of a small gap. Impact velocity was 4.03 km s^{-1} in all simulations.

values of thermal diffusivity (10^{-4}–10^{-5} m^2 s^{-1}) for metals, such localized heat can persist for hundreds to thousands of nanoseconds. The release-affected zones, thus, perturb measurements in a similar manner as the reverberation affected zones found in direct impact experiments.[58]

C. Adhesive decomposition

Virtually, all polymers are known to decompose under shock compression from 20 to 30 GPa.[54] How is it possible that bonded samples above this limit do not show obvious signs of such decomposition? Figure 14 provides some insight on this matter. Glue temperature calculations shown in this plot are based on PMMA described by SESAME 97735.[68] The red curve shows temperatures achieved by single-shock compression (Hugoniot), while the blue curve shows the coolest temperatures attainable under adiabatic conditions (isentrope). All dynamic compression states lie somewhere between these extremes.

Open black circles in Fig. 14 illustrate several examples of multiple shock recompression, the inevitable result of glue between a metal sample and a lithium fluoride window. The connecting lines visually link states for a particular reverberation—the glue experiences only discrete temperature–pressure states, not the continuum of intermediate states. By definition, the first glue shock lies on the Hugoniot, and there is little temperature change on the subsequent shocks. Most calculations shown here (solid lines) are based on an aluminum sample and a LiF window, with one additional case (dotted line) for copper and LiF. General trends are the same in either case, apart from differences in the first shock state for the same final pressure.

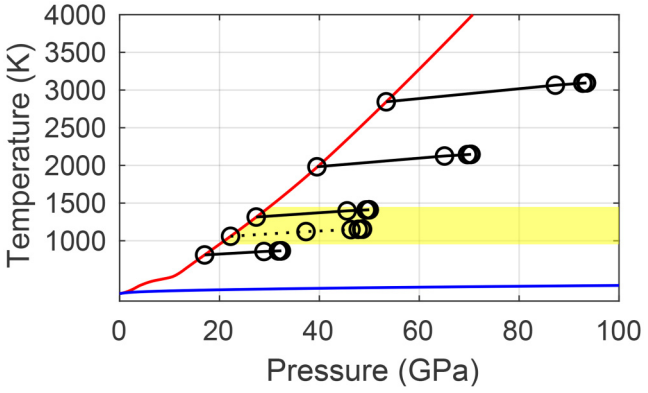

FIG. 14. Calculated glue temperature states.

The yellow-shaded region in Fig. 14 indicates the approximate Hugoniot temperature at the reported 20–30 GPa shock decomposition pressure for polymers, which presumably applies to Loctite as well as any epoxy. The fact that adhesives reverberate within the metal–window stack allows higher pressure to be attained without reaching the necessary temperature to cause decomposition, i.e., adhesive temperature depends primarily on the first shock state. For example, one of the Al–LiF calculations and the Cu–LiF calculation fall within the shaded region. For this particular EOS, decomposition occurs at a maximum temperature of 1450 K on the Hugoniot, but multi-shock compression keeps the glue below this threshold to at least 50 GPa for an Al sample. The final temperature is further reduced for a copper sample, where the first shock is 22 GPa rather than 27 GPa.

Reverberation might explain adhesive function to 60 GPa, but strong evidence of failure was not observed here until $P > 100$ GPa. It could be that decomposition is further suppressed by multiple shocks compared to a single shock. In other words, it may be possible to reach higher temperatures without decomposition by avoiding a single shock—the yellow region in Fig. 14 may not be purely horizontal as shown. Glue thickness presumably plays a strong role as well. In previous studies, the adhesive bonds are quite likely to be $\gg 1\,\mu$m thick, both because of insufficient pressure during assembly and unreliable thickness characterization. A thin decomposing bond has much less effect on pyrometry than a thick bond, both in terms of sample attenuation and self emission. Operating wavelength could also play a role. Bond emission may be limited to shorter wavelengths, where the sample radiance is lower than at longer wavelengths. Bond failure sensitivity is likely also amplified by the high detector gain needed to detect short wavelengths for temperatures $\ll 3000$ K.

VII. CONCLUSIONS

This work established the transparency range of adhesive bonds for radiometric shock temperature studies, compared the results of bonded and gapped temperature experiments under similar conditions, and analyzed the observed differences between

these experiments. These results suggest several guidelines for the design and analysis of shock experiments using the emission of a metal surface across a transparent interface to estimate the metal temperature.

First, it is extremely important to take into account the differences between a bonded sample–window interface and a gapped interface, even when the gap is small. The analysis of temperature from a gapped target requires two substantial corrections with large uncertainties. The first is the well-known thermal diffusion problem of an interface with unknown bulk temperature, thermal effusivity, and boundary conductance. More concerning is the necessary adjustment from the interface temperature to the bulk state far from the interface. The micrometer-thick layer of the interface material undergoing complete pressure release and subsequent reshock is dramatically hotter than the bulk state, systematically biasing radiance measurements and confounding analysis. The extent of this release-affected layer is directly proportional to the width of the initial gap, which can be difficult to determine experimentally, and is often variable across the sample–window interface. Decay of the heated layer in a gapped experiment through thermal diffusion, even with a few-micrometer gap, likely occurs on timescales similar to or longer than the duration of the experiment.

Shock experiments using polymer adhesive layers—under conditions that do not cause failure under compression—alleviate both of these concerns. Our tests show that thermal emission can be collected from sample surfaces that are attached to windows with a bond under a significant range of conditions. Pressing the sample–window assembly with as much force as possible helps to create bonds of $<10\,\mu$m thickness, and radiometric measurements of thin bonds do not seem to show emission in the near-infrared for pressures below 77 GPa, possibly as high as 100 GPa. In addition to Loctite, the common adhesives Stycast, Epotek, and Angstrombond are likely feasible. More importantly, the sample surface temperature is similar to the bulk state due to substantially reduced additional heating generated by the shock-partial release-reshock cycle. For example, Fig. 13 demonstrates that, in our experiments, the sample near the interface is $<5\%$ hotter than the bulk state. Second, the poor conductivity of the compressed polymer, in addition to the poor interface conductance between the polymer and both the sample and the window, likely leaves the sample temperature within the sample skin depth within a few percent of the bulk material.

Measurements of a material with unknown EOS might begin by shocking the glued samples to lower pressures and temperatures at which the glue is very likely not to fail. Experiments can be conducted at increasing pressure until either a dramatic increase in temperature or a measured temperature that does not remain steady under steady compression is observed. Our results provide guidelines for choosing these compression states.

ACKNOWLEDGMENTS

The authors thank Brandon La Lone and Jerry Stevens for their discussion, criticism, and insights regarding the analyses presented in this work. We warmly remember the apostle of glue-bonded shock temperature experiments, David Holtkamp.

Experiments conducted at the STAR facility were made possible by the excellent work of Ryan Zarate, Marcos Vigil, John Martinez, Lena Pacheco, Brent Cockreham, and Christopher Johnson, among others.

Sandia National Laboratories is a multi-mission laboratory managed and operated by National Technology and Engineering Solutions of Sandia LLC, a wholly owned subsidiary of Honeywell International Inc. for the U.S. Department of Energy's National Nuclear Security Administration under Contract No. DE-NA0003525. Nevada National Security Sites is operated by Mission Support and Test Services, LLC for the National Nuclear Security Administration of U.S. Department of Energy under contract No. DE-NA0003624.

AUTHOR DECLARATIONS

Conflict of Interest

The authors have no conflicts to disclose.

Author Contributions

T. M. Hartsfield: Conceptualization (equal); Data curation (equal); Formal analysis (equal); Funding acquisition (equal); Investigation (equal); Methodology (equal); Project administration (equal); Supervision (equal); Validation (equal); Writing – original draft (equal); Writing – review & editing (equal). **K. M. Amodeo:** Conceptualization (equal); Data curation (equal); Formal analysis (equal); Investigation (equal); Methodology (equal); Project administration (equal); Supervision (equal); Validation (equal); Writing – review & editing (equal). **D. Ramsey:** Investigation (equal); Methodology (equal). **D. J. Buckley:** Investigation (equal); Methodology (equal). **L. R. Veeser:** Formal analysis (equal); Investigation (equal); Writing – review & editing (equal). **D. H. Dolan:** Conceptualization (equal); Formal analysis (equal); Funding acquisition (equal); Investigation (equal); Methodology (equal); Software (equal); Validation (equal); Writing – original draft (equal); Writing – review & editing (equal).

DATA AVAILABILITY

The data that support the findings of this study are available from the corresponding authors upon reasonable request.

APPENDIX A: INTERFACE THERMAL PROPERTIES

Analysis of shock temperature on one side of a material interface requires analysis of the initial thermal/mechanical states across the interface and their subsequent diffusion. This appendix describes calculations on two simple model test systems: a sample of Al metal in direct contact with a LiF window and a sample of Al attached to a LiF window with a polymer adhesive bond layer, approximated by polymethylmethacrylate (PMMA). These systems are relatively simple, use common and well-characterized materials, and correspond to the experiments reported in Sec. IV.

1. Experiments without bond layers

Analysis of experiments measuring the temperature of shocked samples in direct contact with an optical window generally

uses the models of Grover and Urtiew.[66,69] They demonstrated that an ideal theoretical interface with perfect boundary conductance between two materials, each with homogeneous post-shock T, density ρ, thermal conductivity κ_T, and specific heat c_p, has a time-independent temperature,

$$T^* = T_1 - \frac{T_1 - T_2}{1 + \alpha}, \tag{A1}$$

where α is defined as the ratio of the thermal effusivities of the materials,

$$\alpha \equiv \sqrt{\frac{\rho_1 \kappa_{T1} c_{p1}}{\rho_2 \kappa_{T2} c_{p2}}}. \tag{A2}$$

In this simple model, the temperature measured at the interface is corrected to infer the sample temperature. Intuitively, and from Eq. (A1), it is clear that the sample temperature correction scales proportionally with the difference in temperature between the sample and the window, $T_1 - T_2$. If the shocked window and the sample possess different temperatures, then $T_1(T^*)$ is a function of T_2 and parameter α, estimated from the combination of six properties of the system under compression. While ρ is generally well constrained, the experimental data on c_p and κ_T do not exist for most materials under most shocked conditions.

Figure 15 displays the relationship of the measured interface temperature to the bulk sample shock temperature as a function of α (blue line). This calculation expresses temperature in absolute form, with $T_1 \equiv 1$ for the sample and $T_2 \equiv 0$ for the window. For typical configurations of metals in contact with optical windows, α is roughly between 1 and 10. Conservative uncertainty ranges in material parameters, particularly in κ_T of the metal and the window, lead to a factor of ~2−−5 uncertainty in α.[40] The points shown in Fig. 15 give mean, high, and low bound estimations for an Al–LiF interface, using approximate parameters[70] in published works.[40,58] These calculations are meant to demonstrate the uncertainty in the Grover calculation and not to define its value for a particular experiment. Plausible experimental uncertainty in thermal conductivity under shock compression and heating of a factor of two (Fig. 15, yellow and purple) cause T^* to vary from about 45%–80% of the difference in T between the sample and the window.

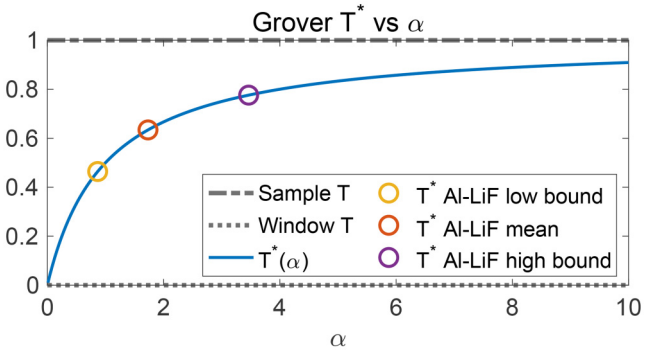

FIG. 15. The ratio of interface temperature (T^*) to absolute metal sample T as a function of α (blue line), where T is expressed on a scale from 0 (window T) to 1 (sample T). The points show an approximate example of mean and bound values for a shocked Sn–LiF interface using the parameter values discussed in Sec. 1 of Appendix A.

Physical interfaces have both finite contact conductance (G_c) and thermal boundary conductance (G_b). Neither of these properties are taken into account in the Grover model. The former results from imperfect physical contact between any real surfaces, increasing with the smoothness of the surfaces and the pressure applied between them.[71,72] The latter results from the limitations in thermal transport between dissimilar materials, i.e., different electron and phonon properties in each material, present even in atomically smooth interfaces.[73] The net inverse conductance (resistance) is a series sum of each effect,

$$\frac{1}{G} \equiv \frac{1}{G_c} + \frac{1}{G_b}. \tag{A3}$$

Even for a perfect contact ($G_c \to \infty$), total conductance at the interface remains finite. The Grover model assumes that G_b also becomes infinite under shock compression.

Transient heat flow between two materials with finite G allows temperature discontinuities to exist, at least for some period of time. The interface will assume an initial temperature between the low bound of the Grover value and the high bound of the sample's bulk shock state. It then equilibrates toward the Grover value on some timescale. Dynamic T calculation is treated numerically here rather than analytically. Figure 8 shows $T(G)$ calculations for Al–LiF, with the parameters given in our previous calculations, performed with a numerical code utilizing the method of lines[74] as described in a previous work.[58] The top panel shows temperature along the compression axis $T(x)$ at $t = 300$ ns; and the bottom panel demonstrates the temperature history $T(t)$ at one location, 20 nm into the sample, approximating the penetration depth of a radiometric measurement. On the few-hundred-ns measurement timescales typical in shock experiments, G must exceed 10^8 (W m^{-2} K^{-1}) for T^* to converge to the infinite conduction approximation, while $G < 10^6$ results in T^* remaining near sample temperature under shock stress.

The experimental values of interface conductance under shock are unknown. Tang used the relaxation of apparent temperature measured in shock experiments[33] to experimentally calculate $G \sim 10^7$ W m^{-2} K^{-1} between shocked sapphire and shocked Fe; however, the darkening sapphire window likely invalidated the radiance measurements. Hohensee studied the conduction between metals and diamond at pressures up to 50 GPa, finding G increasing with pressure but plateauing to ~10^8 W m^{-2} K^{-1}. Hopkins reviewed $G(T)$ at ambient pressure and generally found plateauing increase up to ~500 K, with electrical conductor-to-insulator interfaces ranging from $G < 10^7$ to nearly 10^9. It seems plausible that $G \sim 10^7$−10^8 W m^{-2} K^{-1} for interfaces between shocked metals and LiF. If so, T^* varies from about 65% to 80% of $T_1 - T_2$. The uncertainty in sample temperature inference due to the uncertainty in G appears to be roughly half as large as that caused by the uncertainty in α.

Experimental configurations that place a thin intermediate layer between the sample and the window create a dynamic behavior that is inherently more complex, both thermally and mechanically. Mechanical equilibration of a system including a few-μm layers results in a series of stress states lasting <10 ns. This leaves the loading axis at a non-uniform T that generally requires hydrodynamic simulations with multiphase EOS models to fully characterize.[28,40,58] We analyze this is in Sec. VI B.

Grover analyzed the system of a sample, window, and thin intermediate layer, each starting at a single uniform temperature, with perfect thermal conduction between the layers. Tang analytically added finite boundary conductance and concluded that it created time dependence in the interface temperature.[75] That work estimated a time for interface T to converge to a steady value; the results varied in comparison with the experimental data available at the time. Brantley applied this analysis to experiments using a LiF window sputtered with Sn or Fe and pressed to an Fe plate, estimating that uncertain boundary conductance produced uncertainty in T of up to 15%. Brantley also reported that uncertainty in α causes 10% uncertainty in T. Other experimental uncertainties, including porosity in the sputtered layer and the film-baseplate gap, produced T uncertainty of roughly 1%–10%.

2. Experiments employing adhesive-bonded samples

To similarly analyze thermal diffusion between a metal target bonded to a window, we introduce a thin layer of polymer adhesive to our model Al–LiF system. The ambient density of Loctite is 1.05 g cm^{-3}; shock data[76] on a similar polymer polymethylmethacrylate (PMMA) suggests $\rho = 2.0$ g cm^{-3} at 25 GPa, while experiments and simulations on similar polymers such as polyethylene and polymethylpentene give estimates of $\rho = 1.9$ and 1.6 g cm^{-3}.[5,77] The value 1.8 g cm^{-3} is used here, noting that this uncertainty is small compared to the uncertainty in thermal properties, which have not generally been measured under shock compression.

The adhesive's c_p value under ambient conditions is specified as 0.3 J g^{-1} K^{-1}. Ambient k_T is specified as 0.1 W m^{-2} K^{-1}, which is less than 0.1% of that of an average metal and 1% of LiF, but is comparable to polymer plastics and wood. Andersson experimentally studied PMMA and found that c_p increases moderately with increasing pressure and temperature; the estimate c_p is 0.8 J g^{-1} K^{-1} is used here. Andersson also measured k_T and found moderate increase with increasing pressure and small increase with increasing temperature. Hsieh measured and fitted $k_T(P)$.[78] From the two models, k_T can be estimated as 0.4−0.7 W m^{-2} K^{-1}. Computational studies by Liu suggested that straining polymer chains increased their k_T, possibly implying that shock compression might tamp increases in $k_T(P)$;[79] the value $k_T = 0.6$ W m^{-2} K^{-1} is used here. The adhesive interfaces with Sn and LiF also possess finite G. The interface of an amorphous insulator with a crystalline metal or a crystalline insulator should inherently limit both electrical and phonon conductivities.

Figure 9 shows the results of thermal diffusion simulations including an adhesive layer with the estimated properties. The Sn sample with initial shock T $(T_{\text{shock}}) = 1$, attached with glue $(T_{\text{shock}} = 0.2)$ to a window $(T_{\text{shock}} = 0)$ is allowed to equilibrate for 300 ns, the approximate timescale for most practical shock experiments, with varying interface conductance G. In all cases, the sample T skin depth of the optical pyrometry measurement is between 0.94 and 0.98, i.e., 94%–98% of the difference between the sample and window shock temperatures. In no case does significant heat diffuse from the sample to the window. The T histories at these interfaces are steady to less than 5% and can be described as $T_{\text{sample}} - (0.04 \pm 0.02) \times (T_{\text{sample}} - T_{\text{glue}})$.

Modern experiments measuring radiance and estimating the temperature of shocked metals under steady loading in this configuration report a nearly steady temperature.[8,31,47–50,58] In experiments where dynamic emissivity was measured, a moderate change in measured radiance was often found to be caused by the change in emissivity, not temperature change.[8,49] Steady T_{meas} is indicative of either exceptionally good thermal conduction—the case of $G \to \infty$ demonstrated in Fig. 8 with direct contact between the sample and a LiF crystal—or very poor thermal conduction, as would be expected between a metal and an amorphous insulator as demonstrated in Fig. 9.

REFERENCES

[1]G. Duvall and R. Graham, "Phase transitions under shock wave loading," Rev. Mod. Phys. **49**, 523 (1977).
[2]W. Nellis, "Dynamic compression of materials: Metallization of fluid hydrogen at high pressures," Rep. Prog. Phys. **69**, 1479 (2006).
[3]S. Kormer, M. Sinitsyn, G. Kirillov, and V. Urlin, "Experimental determination of the temperature in shock-compressed NaCl," Sov. Phys. JETP **21**, 689 (1965).
[4]G. Lyzenga and T. J. Ahrens, "Multiwavelength optical pyrometer for shock compression experiments," Rev. Sci. Instrum. **50**, 1421–1424 (1979).
[5]W. Nellis, F. H. Ree, R. Trainor, A. Mitchell, and M. Boslough, "Equation of state and optical luminosity of benzene, polybutene, and polyethylene shocked to 210 GPa (2.1 Mbar)," J. Chem. Phys. **80**, 2789–2799 (1984).
[6]C. Yoo, N. Holmes, M. Ross, D. Webb, and C. Pike, "Shock temperatures and melting of iron at Earth core conditions," Phys. Rev. Lett. **70**, 3931 (1993).
[7]D. Partouche-Sebban, D. Holtkamp, J. Pélissier, J. Taboury, and A. Rouyer, "An investigation of shock induced temperature rise and melting of bismuth using high-speed optical pyrometry," Shock Waves **11**, 385–392 (2002).
[8]B. La Lone, P. Asimow, O. Fat'yanov, R. Hixson, G. Stevens, W. Turley, and L. Veeser, "High-pressure melt curve of shock-compressed tin measured using pyrometry and reflectance techniques," J. Appl. Phys. **126**, 225103 (2019).
[9]G. Lyzenga, T. J. Ahrens, W. Nellis, and A. Mitchell, "The temperature of shock-compressed water," J. Chem. Phys. **76**, 6282–6286 (1982).
[10]N. Holmes, M. Ross, and W. Nellis, "Temperature measurements and dissociation of shock-compressed liquid deuterium and hydrogen," Phys. Rev. B **52**, 15835 (1995).
[11]S.-N. Luo, J. A. Akins, T. J. Ahrens, and P. D. Asimow, "Shock-compressed $MgSiO_3$ glass, enstatite, olivine, and quartz: Optical emission, temperatures, and melting," J. Geophys. Res. Solid Earth **109**, B05205 (2004).
[12]D. Hicks, T. Boehly, J. Eggert, J. Miller, P. Celliers, and G. Collins, "Dissociation of liquid silica at high pressures and temperatures," Phys. Rev. Lett. **97**, 025502 (2006).
[13]A. Seifter, M. Furlanetto, M. Grover, D. Holtkamp, G. Macrum, A. Obst, J. Payton, J. Stone, G. Stevens, D. Swift *et al.*, "Use of IR pyrometry to measure free-surface temperatures of partially melted tin as a function of shock pressure," J. Appl. Phys. **105**, 123526 (2009).
[14]T. M. Hartsfield, R. K. Schulze, B. M. La Lone, J. J. Charonko, J. E. Hammerberg, J. D. Regele, M. M. Schauer, J. D. Schwarzkopf, D. G. Sheppard, G. D. Stevens *et al.*, "The temperatures of ejecta transporting in vacuum and gases," J. Appl. Phys. **131**, 195104 (2022).
[15]G. Maskaly, G. Stevens, B. La Lone, W. Turley, M. Staska, F. Najjar, and T. Hartsfield, "Non-Richtmyer–Meshkov instability ejecta production based on shallow bubble collapse," J. Appl. Phys. **133**, 025901 (2023).

[16]T. M. Hartsfield and K. M. Amodeo, "The platinum liquid-vapor phase boundary mapped by fluid flyer experiments," Phys. Rev. B **111**(13), 134115 (2025).
[17]A. Seifter and A. W. Obst, "About the proper wavelength for pyrometry on shock physics experiments," Int. J. Thermophys. **28**, 934–946 (2007).
[18]J. D. Bass, B. Svendsen, and T. J. Ahrens, "The temperature of shock compressed iron," High Pressure Res. Min. Phys. **39**, 393–402 (1987).
[19]E. Blanco, J. Mexmain, and P. Chapron, "Temperature measurements of shock heated materials using multispectral pyrometry: Application to bismuth," Shock Waves **9**, 209–214 (1999).
[20]P. Héreil and C. Mabire, "Temperature measurement of tin under shock compression," J. Phys. IV France **10**, Pr9-799–Pr9-804 (2000).
[21]B. La Lone, G. Stevens, W. Turley, D. Holtkamp, A. Iverson, R. Hixson, and L. Veeser, "Release path temperatures of shock-compressed tin from dynamic reflectance and radiance measurements," J. Appl. Phys. **114**, 063506 (2013).
[22]J. A. Hawreliak, J. Winey, Y. Toyoda, M. Wallace, and Y. M. Gupta, "Shock-induced melting of [100] lithium fluoride: Sound speed and Hugoniot measurements to 230 GPa," Phys. Rev. B **107**, 014104 (2023).
[23]P. Poulsen, D. Baum, P. Fiske, and D. Holtkamp, "Temperature measurement on shocked surfaces," Technical Report, 2000.
[24]H. Huang, X. Hu, F. Jing, L. Cai, Q. Shen, Z. Gong, and H. Liu, "Melting behavior of Fe-O-S at high pressure: A discussion on the melting depression induced by O and S," J. Geophys. Res. Solid Earth **115**, B05207, https://doi.org/10.1029/2009JB006514 (2010).
[25]G. Hao, F. Liu, D. Zhang, and M. Zhang, "Optical emission of directly contacted copper/sapphire interface under shock compression of megabar," Appl. Phys. Lett. **90**, 261914 (2007).
[26]D. Hare, N. Holmes, and D. Webb, "Shock-wave-induced optical emission from sapphire in the stress range 12 to 45 GPa: Images and spectra," Phys. Rev. B **66**, 014108 (2002).
[27]O. Fat'Yanov, R. Webb, and Y. Gupta, "Optical transmission through inelastically deformed shocked sapphire: Stress and crystal orientation effects," J. Appl. Phys. **97**, 123529 (2005).
[28]R. Hixson, S. Thomas, B. LaLone, W. Turley, M. Hawkins, and G. Stevens, "Strategic studies in dynamic material response of weapons-relevant materials," Technical Report, 2021.
[29]S. Liu, J. Li, J. Li, T. Xue, T. Tao, H. Ma, X. Wang, J. Weng, and Z. Li, "Simultaneous measurement of the dynamic emissivity and the radiance of the shocked Al/LiF interface in the near-infrared wavelength," Rev. Sci. Instrum. **89**, 044903 (2018).
[30]J. Li, Q. Wu, J. Li, T. Xue, Y. Tan, X. Zhou, Y. Zhang, Z. Xiong, Z. Gao, and T. Sekine, "Shock melting curve of iron: A consensus on the temperature at the Earth's inner core boundary," Geophys. Res. Lett. **47**, e2020GL087758, https://doi.org/10.1029/2020GL087758 (2020).
[31]Y. Zhang, Y. Tan, H. Y. Geng, N. P. Salke, Z. Gao, J. Li, T. Sekine, Q. Wang, E. Greenberg, V. B. Prakapenka *et al.*, "Melting curve of vanadium up to 256 GPa: Consistency between experiments and theory," Phys. Rev. B **102**, 214104 (2020).
[32]Q. Williams, R. Jeanloz, J. Bass, B. Svendsen, and T. J. Ahrens, "The melting curve of iron to 250 gigapascals: A constraint on the temperature at Earth's center," Science **236**, 181–182 (1987).
[33]W. Tang, F. Jing, R. Zhang, and J. Hu, "Thermal relaxation phenomena across the metal/window interface and its significance to shock temperature measurements of metals," J. Appl. Phys. **80**, 3248–3253 (1996).
[34]P. Rigg, M. Knudson, R. Scharff, and R. Hixson, "Determining the refractive index of shocked [100] lithium fluoride to the limit of transmissibility," J. Appl. Phys. **116**, 033515 (2014).
[35]O. L. Anderson and A. Duba, "Experimental melting curve of iron revisited," J. Geophys. Res. Solid Earth **102**, 22659–22669, https://doi.org/10.1029/97JB01641 (1997).
[36]M. J. Brown, "The equation of state of iron to 450 GPa: Another high pressure solid phase?" Geophys. Res. Lett. **28**, 4339–4342, https://doi.org/10.1029/2001GL013759 (2001).
[37]D. Alfè, G. Price, and M. Gillan, "Iron under Earth's core conditions: Liquid-state thermodynamics and high-pressure melting curve from *ab initio* calculations," Phys. Rev. B **65**, 165118 (2002).
[38]J. H. Nguyen and N. C. Holmes, "Melting of iron at the physical conditions of the Earth's core," Nature **427**, 339–342 (2004).
[39]B. Svendsen, J. D. Bass, and T. J. Ahrens, "Optical radiation from shock-compressed materials and interfaces," Phys. Rep. **180**, 333–416 (1989).
[40]D. A. Brantley, R. S. Crum, and M. C. Akin, "Comparing temperature convergence of shocked thin films of tin and iron to a bulk temperature source," J. Appl. Phys. **129**, 015903 (2021).
[41]C. Dai, J. Hu, and H. Tan, "Hugoniot temperatures and melting of tantalum under shock compression determined by optical pyrometry," J. Appl. Phys. **106**, 043519 (2009).
[42]A. Dewaele, M. Mezouar, N. Guignot, and P. Loubeyre, "High melting points of tantalum in a laser-heated diamond anvil cell," Phys. Rev. Lett. **104**, 255701 (2010).
[43]C. Dai, X. Jin, X. Zhou, J. Liu, and J. Hu, "Sound velocity variations and melting of vanadium under shock compression," J. Phys. D: Appl. Phys. **34**, 3064 (2001).
[44]J. Johnson and L. Barker, "Dislocation dynamics and steady plastic wave profiles in 6061-T6 aluminum," J. Appl. Phys. **40**, 4321–4334 (1969).
[45]L. M. Barker and R. Hollenbach, "Shock-wave studies of PMMA, fused silica, and sapphire," J. Appl. Phys. **41**, 4208–4226 (1970).
[46]S. Stewart, G. Kennedy, L. Senft, M. Furlanetto, A. Obst, J. Payton, and A. Seifter, "Post-shock temperature and free surface velocity measurements of basalt," in *AIP Conference Proceedings* (American Institute of Physics, 2006), Vol. 845, pp. 1484–1487.
[47]T. A. Ota, R. Amott, C. Carlson, D. J. Chapman, M. A. Collinson, R. Corrow, D. E. Eakins, T. Graves, T. Hartsfield, D. B. Holtkamp *et al.*, "Comparison of simultaneous shock temperature measurements from three different pyrometry systems," J. Dyn. Behav. Mater. **5**, 396–408 (2019).
[48]B. Jensen, T. Hartsfield, D. Holtkamp, F. Cherne, R. Corrow, T. Graves, and A. Iverson, "Examining the high-pressure response and shock melting in cerium using optical pyrometry," Phys. Rev. B **102**, 214105 (2020).
[49]R. Hixson, B. La Lone, M. Staska, G. Stevens, W. Turley, and L. Veeser, "Temperature measurements in cerium shocked from 8.4 to 23.5 GPa," J. Appl. Phys. **129**, 155106 (2021).
[50]S. Duwal, C. A. McCoy, D. H. Dolan III, C. A. Melton, M. D. Knudson, S. Root, R. Hacking, B. Farfan, C. Johnson, C. S. Alexander *et al.*, "Samarium: From a distorted-fcc phase to melting under dynamic compression using in-situ x-ray diffraction," Sci. Rep. **12**, 16777 (2022).
[51]T. M. Hartsfield and D. Dolan, "Establishing temperature from radiance of dynamically compressed metals," J. Appl. Phys. **131**, 185901 (2022).
[52]D. Partouche-Sebban, J. Pélissier, F. Abeyta, W. Anderson, M. Byers, D. Dennis-Koller, J. Esparza, R. Hixson, D. Holtkamp, B. Jensen *et al.*, "Measurement of the shock-heated melt curve of lead using pyrometry and reflectometry," J. Appl. Phys. **97**, 043521 (2005).
[53]M. Akin and R. Chau, "The suitability of Loctite 326 for thermal emission measurements," J. Dyn. Behav. Mater. **2**, 421 (2016).
[54]D. Dattlebaum and J. Coe, "Shock-driven decomposition of polymers and polymeric foams," Polymers **11**, 493 (2019).
[55]W. W. So and C. C. Lee, "Fluxless process of fabricating In-Au joints on copper substrates," IEEE Trans. Compon. Packag. Technol. **23**, 377–382 (2000).
[56]D. A. Boness, "Thermal relaxation of CsI shocked to 45 GPa, with a LiF window, and optical characterization of LiF shocked to 85 GPa," in *AIP Conference Proceedings* (American Institute of Physics, 2012), Vol. 1426, pp. 1605–1608.
[57]B. La Lone, D. Turley, G. Stevens, G. Capelle, E. Larson, M. Grover, L. Veeser, O. Fatyanov, and P. Asimowc, "New methods to quantify thermodynamic and phase properties of shocked materials," Site-Directed Research and Development No. 11, 2015.
[58]T. Hartsfield, B. La Lone, G. Stevens, L. Veeser, and D. Dolan, "Thermal interfaces in dynamic compression experiments," J. Appl. Phys. **128**, 015903 (2020).

[59]T. Hartsfield, B. La Lone, G. Stevens, M. Beason, J. Baldwin, and W. Turley, "Temperature, enthalpy, and kinetics of cerium resolidification under dynamic compression," Phys. Rev. B **108**, L140101 (2023).
[60]O. Strand, D. Goosman, C. Martinez, T. Whitworth, and W. Kuhlow, "Compact system for high-speed velocimetry using heterodyne techniques," Rev. Sci. Instrum. **77**, 83108 (2006).
[61]B. Marshall, "Glue film thickness measurements by spectral reflectance," Technical Report, 2010.
[62]R. Hooke, *Micrographia* (The Royal Society, London, 1665).
[63]D. H. Dolan, T. Ao, and S. C. Grant, "The Sandia Matlab analysis hierarchy (SMASH) toolbox," Technical Report, 2016.
[64]T. Sjostrom, S. Crockett, and S. Rudin, "Multiphase aluminum equations of state via density functional theory," Phys. Rev. B **94**, 144101 (2016).
[65]P. C. Myint, E. L. Shi, S. Hamel, H. Cynn, Z. Jenei, M. J. Lipp, W. J. Evans, and M. C. Akin, "Two-phase equation of state for lithium fluoride," J. Chem. Phys. **150**, 074506 (2019).
[66]R. Grover and P. Urtiew, "Thermal relaxation at interfaces following shock compression," J. Appl. Phys. **45**, 146 (1974).
[67]J. M. McGlaun, S. Thompson, and M. Elrick, "CTH: A three-dimensional shock wave physics code," Int. J. Impact Eng. **10**, 351–360 (1990).
[68]J. D. Coe, M. Lentz, K. A. Velizhanin, J. T. Gammel, J. Kaushagen, K. Jones, and K. R. Cochrane, "The equation of state and shock-driven decomposition of polymethylmethacrylate (PMMA)," J. Appl. Phys. **131**, 125108 (2022).
[69]P. Urtiew and R. Grover, "Temperature deposition caused by shock interactions with material interfaces," J. Appl. Phys. **45**, 140 (1974).
[70]$\rho = 3.8\,\mathrm{g\,cm^{-3}}$, $\kappa_T = 200\,\mathrm{W\,m^{-1}\,K^{-1}}$, and $c_p = 0.2\,\mathrm{J\,g^{-1}\,K^{-1}}$ for Al and $\rho = 2.6\,\mathrm{g\,cm^{-3}}$, $\kappa_T = 10\,\mathrm{W\,m^{-1}\,K^{-1}}$, and $c_p = 1.9\,\mathrm{J\,g^{-1}\,K^{-1}}$ for LiF.
[71]R. Jacobs and C. Starr, "Thermal conductance of metallic contacts," Rev. Sci. Instrum. **10**, 140 (1939).
[72]A. Tariq and M. Asif, "Experimental investigation of thermal contact conductance for nominally flat metallic contact," Heat Mass Transfer **52**, 291 (2016).
[73]E. T. Swartz and R. O. Pohl, "Thermal boundary resistance," Rev. Mod. Phys. **61**, 605 (1989).
[74]J. VonNeumann and R. D. Richtmyer, "A method for the numerical calculation of hydrodynamic shocks," J. Appl. Phys. **21**, 232–237 (1950).
[75]W. Tang, R. Zhang, F. Jing, and J. Hu, "Restudy on the thermal relaxation at interfaces following shock compression," in *AIP Conference Proceedings* (American Institute of Physics, 1996), Vol. 370, pp. 279–282.
[76]S. P. Marsh, *LASL Shock Hugoniot Data* (University of California Press, 1980), Vol. 5.
[77]T. R. Mattsson, J. M. D. Lane, K. R. Cochrane, M. P. Desjarlais, A. P. Thompson, F. Pierce, and G. S. Grest, "First-principles and classical molecular dynamics simulation of shocked polymers," Phys. Rev. B **81**, 054103 (2010).
[78]W.-P. Hsieh, A. S. Lyons, E. Pop, P. Keblinski, and D. G. Cahill, "Pressure tuning of the thermal conductance of weak interfaces," Phys. Rev. B **84**, 184107 (2011).
[79]J. Liu and R. Yang, "Tuning the thermal conductivity of polymers with mechanical strains," Phys. Rev. B **81**, 174122 (2010).